Optimization of Kerosene Aromatization over Ni/HY Catalysts Using Response Surface Methodology

Saidi, Elham; Ziarati, Mahmoud*[+]; Dehghani, Hossein
Faculty of Chemistry and Chemical Engineering, Malek Ashtar University of Technology,
P.O. Box 15875-1774 Tehran, I.R. IRAN

Khandan, Nahid
Department of Chemical Technologies, Iranian Research Organization for Science and Technology (IROST),
P.O. Box 33535111 Tehran, I.R. IRAN

ABSTRACT: *In this paper, several Ni/Y catalysts were prepared to perform kerosene aromatization. The Na^+ cation of Y zeolite was exchanged with NH_4^+, and then Ni/HY catalysts were synthesized through the precipitation-deposition method. The properties of the samples were characterized by XRD, EDX, and BET. In addition, the Response Surface Method in combination with a three-factor Central Composite Design was employed to optimize the conditions of the reaction over Ni/HY catalysts. The three independent variables were: Ni content of the catalysts, reaction time, and temperature. Analysis of aromatic yield as the response was performed to survey the importance of these independent variables. Results of numerical optimization revealed that maximum operation conditions were 5%Ni-loading at a temperature 450ºC and a reaction time of 120min, in which aromatic yield was 55.74%. This was in agreement with the predicted aromatic content (52.62%) in this condition. Acceptable value for correlation coefficient (R_2= 0.989), root mean square error (RMSE = 0.77), and standard error of prediction (SEP = 1.82) was obtained. These low values confirmed the adequacy and statistical significance of the model to predict an adequate response.*

KEYWORDS: *Y zeolite; Response surface method; Optimization; Aromatization reaction.*

INTRODUCTION

All oil-based fuels contain four main compositions namely alkanes, isoalkanes, naphthenes, and aromatics [1]. Among them, aromatic content has stringent limitations on specifications of hydrocarbon fuels, which is usually limited to <20 or 25 vol. % in many fuels. Meeting this requirement is necessary to decrease the levels of carbon deposits [2]. However, fuels with a low content of aromatics cannot swell the elastomer materials, which can lead to leakage in the engine seals [3]. Moreover, the high content of aromatics, as an organic raw material, is important in petrochemical industries to produce the commercial aromatics used in several applications such as polyester fiber, pesticides, and medicine dyes [4]. Aromatics contribute to 50-80% of the FCC products

***** *To whom correspondence should be addressed.*
+ *E-mail: maziarati@mut.ac.ir*
1021-9986/2022/8/2693-2703 *11/$/6.01*

in the oil refineries [5]. As mentioned in the literature, some researchers prefer the application of higher boiling-point fractions such as gas oil and kerosene for aromatic production instead of expensive light fuels [6].

Numerous papers in the literature study aromatization of hydrocarbon fuels [7-9]. A review indicates a well-designed reaction is necessary to produce the maximum content of aromatics in products. Catalytic reactions act more efficiently than non-catalytic pyrolysis reactions [10]. Processes easily go toward the desired reactions when a highly active catalyst was applied [11].

As recent studies have indicated, each zeolite can provide an individual product, because of its unique properties such as high surface area, porosity, acidity power, environmentally friendly, low cost, etc. [12,13]. Zeolites have been applied as attractive supports in many real processes of the oil refineries such as fluid catalytic cracking (FCC), distillate dewaxing by cracking, hydrocracking, lube dewaxing by isomerization or cracking, gasoline desulfurization, distillate dewaxing by isomerization, light paraffin isomerization, reformate upgrading, and diesel aromatics saturation [14]. According to the literature, Y zeolite is also characterized by high alkane and low aromatic selectivity [15]. Introducing small amounts of metal into a catalyst facilitates the proceeding of reactions towards desirable routes. Nickel is among the commonly used metals because it is cheaper than noble metals and more available than many other metals [16,17]. Another reason for its higher preference is the strong nickel-support interaction in the catalyst that helps prevent nickel sintering and carbon deposition, which has both technical and economic benefits [18,19].

In general, both catalyst and operation conditions affect product quality [20,21]. For instance, increasing the temperature influences catalyst deactivation. It generates more gaseous product fractions and reduces the liquid hydrocarbon. On the other hand, zeolite acid strength creates changes in product composition. Many studies discuss the effect of reaction conditions on product quality [22]. They mostly used classic methods that only change one parameter coincidently, which rarely results in the successful exploration of the interactions of process conditions [23]. Instead, more resources are used and less output production occurs because of non-optimized reactions [24]. To overcome these obstacles, it is necessary to model and optimize key parameters of the reactions. One of the aims of this study is to construct a bridge between modeling and catalytic reforming.

Many methods have been proposed for process modeling and optimization. However, some of these methods present drawbacks. They may not consider the interaction influence of parameters on the response or even miss the optimization of set points. Instead, the Response Surface Method (RSM) can predict accurately complex nonlinear processes. Based on the RSM data, suitable mathematical models can be developed with minimum process knowledge of the given system. One reason is the RSM's ability to save time and lower the cost of experiments [23]. The first people who developed the RSM were *Box* and *Wilson* [25]. They described it as a collection of mathematical and statistical techniques to build an empirical model. This method is an effective technique for statistical modeling and multiple regression analysis of complex processes. It can develop, improve and optimize the process if it finds an accurate relationship between the response and independent variables [26-28].

According to the literature, various factors affect the performance of catalytic aromatization. Effective parameters recorded in previous studies include the percent of metal loading in the catalyst, various material ratios, reaction time, temperature, pressure, and Liquid Hourly Space Velocity (LHSV) [29-33]. Among these parameters, metal content, reaction time, and temperature were the parameters that had the most effect on the catalytic performance of the reforming process [33].

In this original study, the Central Composite Design (CCD) was combined with RSM to predict the effect of the process parameters on the kerosene aromatization as an original study and determine the interactions of the independent variables to optimize the response.

EXPERIMENTAL SECTION

Catalyst preparation

To prepare the Ni/Zeolite catalysts, Nickel nitrate hexahydrate ($Ni(NO_3)_2.6H_2O$), sodium carbonate (Na_2CO_3), and ammonium nitrate (NH_4NO_3) were purchased from the Merck Company (Germany), and the commercial Y zeolite (Si/Al=5.1 in Na-form, surface area $900 m^2/g$) was supplied by the Zeolyst Company (USA).

To obtain the H^+-form of cation in the Y zeolite, the Na-form zeolite was ion-exchanged to NH_4^+ with 0.1mol/L NH_4NO_3 solution. In detail, the solution was aged

at 70ºC for 2h, filtered, and washed with distilled water. Then, the obtained precipitate was dried at 110ºC for 12h and calcined at 550ºC for 4h in air. The prepared powder has the capability of application as support to the catalysts.

Different Ni/Y catalysts were prepared through the Deposition-Precipitation (DP) method. The procedure of this method was approximately the same as described in the literature [34, 35]. In detail, appropriate weights of 1M metal nitrate (Ni $(NO_3)_2.6H_2O$) and sodium carbonate solutions (Na_2CO_3) were added simultaneously to 320ml deionized water at 70ºC and continually stirred by a laboratory magnetic stirrer operated at 700rpm. The flow rate of the basic sodium carbonate solution was adjusted to about 1ml/min to control the pH of the solution around 7±0.2. After that, the sample was aged at the same temperature for 0.5h under slow stirring at a rate of 300rpm. Then, the solution was filtrated, washed three times with deionized water at 70ºC, and added to the suspension of Y zeolite to introduce Ni on the zeolite. The mixtures were stirred, filtered, dried at 110ºC in air overnight, and finally the obtained precipitate was calcined at 550ºC in airflow for 4h.

Catalyst characterization

The X-Ray powder Diffraction (XRD) data were recorded with a Philips PW-3710 diffractometer using a Cu Ka source (λ = 1.5418 °A) in a 2θ range of 5-80° with a scan speed of 10º /min. To identify the diffraction patterns, they were compared with those of known structures in the joint committee of powder diffraction standards (JCPDS) database. The formation of the cubic phase of NiO (JCPDS Card 47-1049) with lattice constant, a = 4·1771Å, was investigated through the XRD pattern, in which distinct peaks at 2θ of 37.26º, 43.29º, 62.88º, 75·42º, and 79.41º were identified as peaks of cubic NiO crystals with various diffraction planes (111), (200), (220), (311) and (222), respectively. The surface area of the samples was calculated by nitrogen physisorption analysis on a CHEMBET-3000 surface characterization analyzer from the Quantachrome Instruments Company (at -77 K). The total surface area was obtained by the Brunauer-Emmett-Teller (BET) equation, while relative pressure (P/P_0) ranged from 0.005 to 0.1. The t-plot method was applied to survey the microporous characteristics. The chemical composition of zeolites in the prepared samples was measured through the Inductively Coupled Plasma (ICP). Ni content in the samples was determined using the Energy-Dispersive X-ray spectrometer (EDX, Zeiss Gemini Leo 1530).

Catalytic aromatization test

In this study, kerosene was applied as the feedstock. It was supplied by the Tehran Oil Refinery Company (TORC) and its specifications are reported in Table 1.

As shown in Fig. 1, an experimental setup was designed and assembled for the aromatization of kerosene. The fixed-bed reactor in this reaction test was made of stainless steel with a height of 150mm and an inner diameter of 10mm (ID=10mm).

To perform the aromatization reaction, 1g of the catalyst (20-40 mesh) was first uniformly loaded in the reactor. Before starting the reaction, the catalyst was reduced at 300 ºC for 1h in pure H_2 with a flowrate of 50 mL/min. Then, the temperature was increased to 450 ºC, and kerosene was passed through the reactor at a flow rate of 5mL/min. The analysis of liquid products was carried out using an Agilent 6890N Gas Chromatography (GC) equipped with a DH capillary column (40m) and Flame Ionization Detector (FID). The injection temperature was set to 300˚C. The column temperature was initially increased from 40 to 100˚C (heating rate of 2˚C/min), then increased to 300˚C (heating rate of 10˚C/min) and maintained for 8min.

The area percentage of each component was calculated as $x_{area\%}$ (Eq. (1)) after identifying the components in the GC-FID.

$$x_{area\%} = \frac{x_{identified\ area}}{\sum x_{area}} \times 100 \quad (1)$$

Where $x_{area.\%}$ was the percentage of the component area in GC [36].

Experimental design and statistical analysis

The RSM, a set of mathematical and statistical techniques, was applied to optimize the combination of operational parameters by reducing and simplifying the experimental designs and statistical analysis [37]. The resulting aromatic yield in the liquid products was then modeled by a CCD with three independent variables. To minimize the block effect, the value of α was set to 1. As shown in Table 2, the different values of the independent variables were as follows: Ni content (0, 5, and 10wt. %),

Table 1: Specifications of supplied kerosene by TORC.

Property	Test method (ASTM)	Feed properties
Density at 15.6 ˚C (kg/m^3)	D 1298	797.4
Distillation IBP (˚C) 185 ˚C (Vol. %) 200 ˚C (Vol. %) 210 ˚C (Vol. %) 235 ˚C (Vol. %) FBP (˚C) Residue (Vol. %)	D 86	 156 ˚C 23.9 48.4 64.1 90.9 260 ˚C 0.81
Sulfur (wt. %)	D 1552	0.007
Flash point	D 3828	50
Freezing point	D 2386	-52
Aromatic content (Vol. %)	D 6379	21.3

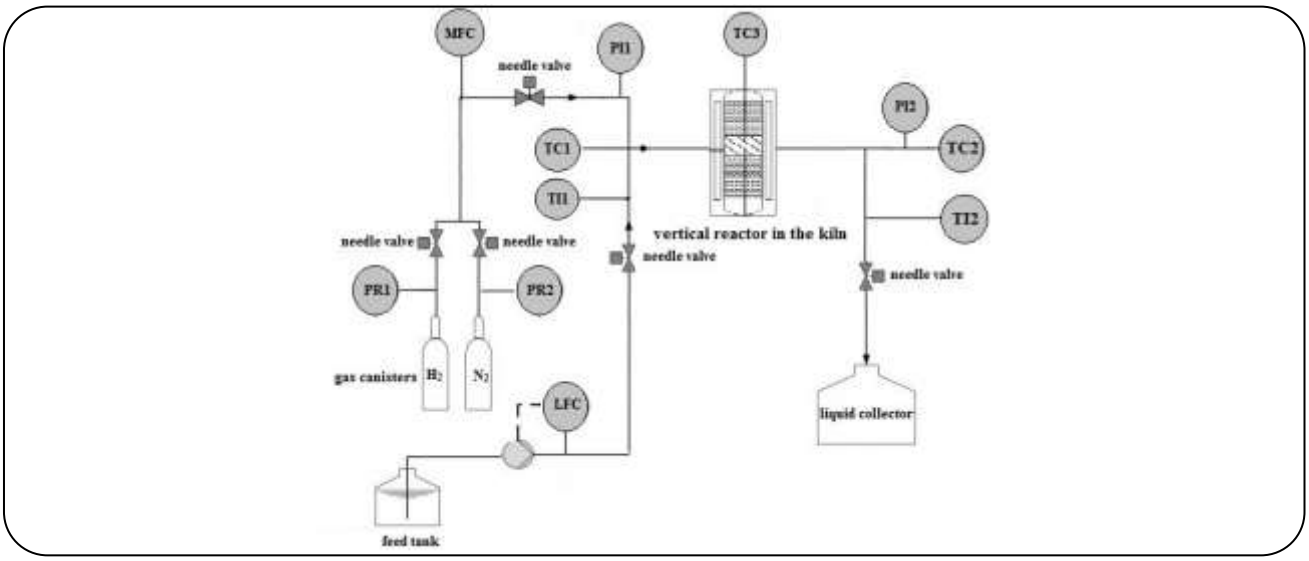

Fig. 1: Schematic diagram of the experimental setup of aromatization: LFC- liquid flow controller; MFC- mass flow controller; TC-thermocouple; TI– temperature indicator; PI – pressure indicator; PR – pressure regulator.

reaction time (0, 120, and 240min), and temperature (250, 350, and 450ºC).

As shown in Eq. (2), the experimental data from the CCD was analyzed using regression (Design Expert™ 11.0) and then fitted to a second-order polynomial model. This equation identified all possible interactions of the selected factors with a response function (Eq. (2)).

$$Y = b_0 + \sum_{i=1}^{k} b_i x_i + \sum_{i=1}^{k} b_{ii} x_i^2 + \sum_{i=1}^{k} \sum_{i=j}^{k} b_{ij} x_i x_j + c \quad (2)$$

Where, *Y* is the response (compositions) and b_0, b_i, b_{ii}, and b_{ij} are the regression coefficients obtained for the constant, linear, quadratic, and interaction terms, respectively. *xi* and *xj* are the independent variables, and *i* and *j* are the linear and quadratic coefficients, respectively. *b* is the regression coefficient, *k* is the number of factors studied and optimized in the experiment, and *c* is the random error.

First, ANOVA (Analysis of Variance) was applied to check the statistical significance of the regression terms. It can evaluate the model coefficients, F-values, significant probabilities, and R^2-values. Then, the adequacy of the regression models was checked by both the F statistic and a lack-of-fit test. This was necessary due to an insignificant lack of fit (p-value > 0.05). Next, the normal probability plots versus the predicted responses were compared to the test

Table 2: Range of independent variables employed for CDD.

Independent variables	Symbols	-1	0	1
Ni content	A	0	5	10
Reaction time	B	0	120	240
Temperature	C	250	350	450

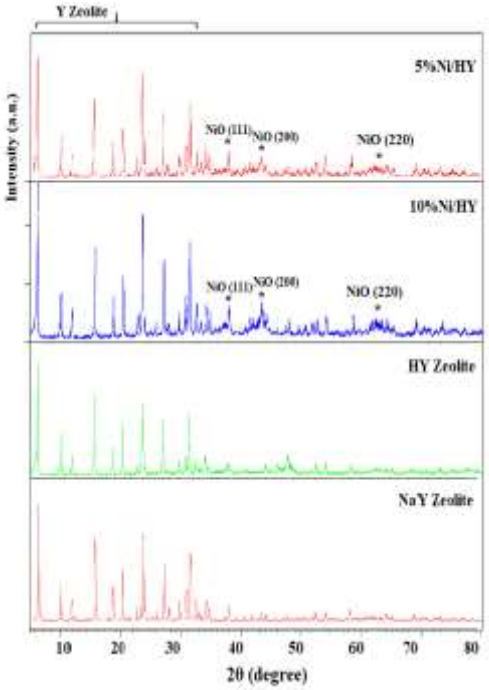

Fig.2: XRD patterns of the parent Y zeolites and the prepared catalysts.

the adequacy of the model [38]. Finally, the surface plots indicated the relationship between the response variable to the independent variables.

RESULTS AND DISCUSSION

The results of catalyst characterization

XRD results

The X-Ray powder Diffraction (XRD) patterns of the parent Y zeolites and the prepared Ni/HY catalysts are displayed in Fig. 2. Both prepared catalysts and parent zeolites display the characteristic XRD patterns of the Y structure. Therefore, the zeolite structure seems not to have been destroyed by the introduction of the nickel, although its crystallinity was slightly changed by the synthesis. The formation of a cubic phase in NiO at 2θ of 37.26º, 43.29º, and 62.88º are identified by asterisks in Fig. 2.

Nanoparticles are characterized by a significant amount of line broadening in the XRD patterns. As shown in Eq. (3), the crystal size can be calculated by using the Debye-Scherer formula [39].

$$D = \frac{\kappa\lambda}{\beta COS\theta} \quad (3)$$

Where k=0.89, λ was the wavelength of the Cu-Kα radiations, β was the full width at half maximum (FWHM) and θ was the angle obtained from 2θ values corresponding to the maximum intensity peak in the XRD pattern.

In general, there is a direct relationship between the peak breadths of a specific phase of material to the mean crystallite size of that material [40]. The crystallite size of the samples was determined using the Scherrer equation and the results are presented in the last column of Table 3. These calculated sizes confirmed that the NiO was highly crystalline according to the XRD data.

The inter-planar space of the prepared catalysts was calculated using Bragg's Law according to Eq. (4) [41].

$$2d\sin\theta = n\lambda \quad (4)$$

Where *n* was considered 1. The average value of *d* for the most intense peak (2θ of 43.29) of all prepared catalysts was 2.06Å (in the range of 1.93 to 2.16). Therefore, the obtained diffraction peaks from X-ray data met the requirements of the standard pattern for NiO [42].

EDX results

As indicated in the 6th column of Table 3, the maximum deviation of Ni content in the catalysts was 0.3%, which indicates a proper approximation of theoretical Ni loading.

BET results

The results of textural properties for the parent Y zeolites and the Ni/Y catalysts were determined by N_2 adsorption-desorption and are indicated in Table 3.

As shown in the 4th column of Table 3, the average pore diameter was around 2–2.4 nm, which is suitable for the performance of kerosene aromatization, because large molecules in the feed could easily reach acid sites in the catalysts. The BET surface area and pore volume were more in the 5%Ni/Y catalyst, which indicated that the Ni particles might cover the porous spaces of the HY sites and as a result decrease both surface area and pore volume.

Table 3: The results of textural analysis for the prepared catalysts.

Row	Catalyst	S_{BET} (m^2/g) [(a)]	Average pore diameter (nm)	V_{total} (cm^3/g) [(b)]	Ni Content [(c)]	Acidity (mmol/g) [(d)]	Crystallite size of Ni (nm) [(e)]
1	NaY	829	2.03	0.32	---	2.54	---
2	HY	733	2.29	0.38	---	2.92	---
3	5%Ni/HY	603	2.37	0.35	5.2	2.87	7.26
5	10%Ni/ HY	536	2.32	0.27	10.1	2.79	8.98

(a) BET surface area (m^2/g); (b) Total pore volume (cm^3/g); (c) obtained from EDX; (d) identified by ICP, (e) calculated by Scherrer equation.

The aromatization reaction was performed for 4h at temperatures of 250, 350, and 450ºC in the presence of Ni/HY catalysts. The liquid products were collected at the end of the reaction and analyzed by GC-FID. All components of the kerosene feedstock and reformed produced liquids were identified or organized by hydrocarbon groups and their carbon atom number C_n. It is noticeable that the catalyst with 5%Ni produced more aromatic content compared with the 10%Ni, which might be due to the occupation of acid sites by Ni particles in the catalyst.

Statistical analysis results of the Central Composite Design (CCD)

Central Composite Design (CCD) results were applied to model the aromatization of kerosene over Ni/HY catalysts and to investigate the effect of the process parameters on aromatic yield in the liquid products.

The signal-to-noise ratio is desirable when it is greater than 4. This ratio was measured by adequate precision and was found to be 29.767 in this model, which indicated an adequate signal to navigate the design space by the model.

Fig. 3 shows no significant difference between the actual and predicted aromatic yield, which is in agreement with the data in columns 5 and 6 of Table 4.

The results obtained by the ANOVA test presented Table 5, show that the three independent variables (Ni content, time reaction, and temperature) were significantly predicted at three different levels, which went to a total of 15 runs (5 of the 20 runs were repetitive). To minimize the block effect, the value of α was set to 1. Hence, a design matrix of experimental runs for different conditions of the independent parameters could be obtained.

According to the value of the R-squared statistic [43], the compatibility was more than 98.99% with the experimental data. This means that the model explained 98.99% of the aromatic yield in this case. Adjusted R-squared was applied to correct the R-squared value for the sample size. This was used to evaluate the model's adequacy and fitness. The value of the adjusted R- squared (0.9809) indicates the significance of the model. Moreover, the predicted R-squared (0.9213) with a difference of only 0.0596 (less than 0.2) was in reasonable agreement with the Adjusted R-square value of 0.9809. Therefore, the Adjusted R-square value showed a 98.09% of confidence level for the results of the variance analysis (ANOVA) in the case of aromatic yield.

A p-value of more than 0.1 was ignored in this model. Therefore, the obtained Eq. (4) could be used to model the aromatic yield. As shown in Table 5, the second-order polynomial equation was coincident with the experimental results.

$$\text{Aromatic yield } (\%) = 45.70 + 9.86A + 1.49B + 6.11C + 4.32AC - 17.27A2 \quad (4)$$

As Eq. (4) shows, the reaction time had less significance in comparison with Ni content and temperature. The significance of the model was implied by the F-value of 109.44, which was obtained in the ANOVA result for the aromatic yield. Therefore, there was only a 0.01% chance that such a large F-value is due to noise.

Fig. 4 (a, b, and c) presents the evaluated properties through 3-D plots of the aromatic yield. Fig. 4a shows the effect of Ni content and reaction time on the performance of aromatic yield at 350ºC. According to the results on response surfaces of aromatic yield, a local maximum point existed in the case of aromatic yield concerning the Ni content of the catalyst. An increase in the Ni-loading up to the optimum point was led to an increase in the aromatic yield to a maximum level, while further increase in the Ni content reversed the trend. The regression results showed that the optimal values of X_1 and X_2 were 120min for the reaction time and 5% for the Ni-content. The predicted value of the aromatic yield was 45.70%.

Table 4: Central Composite Design Matrix and experimental results.

Runs	Independent variables			Aromatic yield	
	Ni content (X_1)	Reaction time (X_2)	Temperature (X_3)	Actual value	Predicted value
1	5	0	350	43.37	44.22
2	5	120	350	45.85	45.70
3	0	0	250	17.26	16.32
4	0	0	450	19.69	20.07
5	5	120	450	55.74	52.62
6	0	240	450	21.23	22.27
7	10	0	450	46.96	47.83
8	10	0	250	27.94	26.79
9	5	240	350	47.60	47.19
10	5	120	250	36.83	40.39
11	10	240	250	31.04	30.55
12	0	120	350	18.05	18.57
13	0	240	250	19.84	18.86
14	10	240	450	50.41	51.25
15	10	120	350	38.37	38.29

Table 5: Results of ANOVA for the aromatic yield.

Source	Sum of squares	df	Mean square	F-value	p-value	
Model	2929.03	9	325.45	109.44	< 0.0001	significant
A-Ni content	972.91	1	972.91	327.15	< 0.0001	significant
B-Reaction time	22.17	1	22.17	7.45	0.0212	significant
C-Temperature	373.62	1	373.62	125.63	< 0.0001	significant
AB	0.7477	1	0.7477	0.2514	0.6269	
AC	149.43	1	149.43	50.25	< 0.0001	significant
BC	0.0593	1	0.0593	0.0199	0.8906	
A^2	820.08	1	820.08	275.76	< 0.0001	significant
B^2	0.0001	1	0.0001	0.0000	0.9953	
C^2	1.79	1	1.79	0.6021	0.4557	
Residual	29.74	10	2.97			
Lack of Fit	29.74	5	5.95			
Pure Error	0.0000	5	0.0000			
Cor Total	2958.77	19				

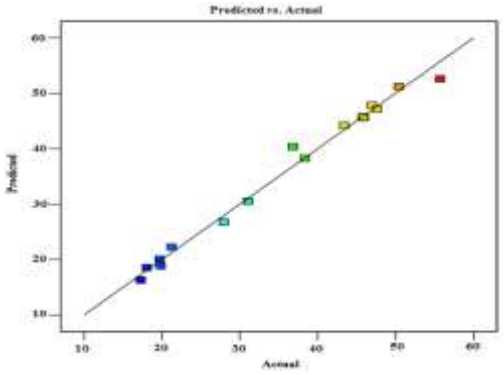

Fig. 3: Predicted aromatic yield versus actual data.

Fig. 4b provides the effect of the Ni content of the catalyst and reaction temperature on the aromatic yield. An increase in temperature and the Ni content of the catalyst up to 5%Ni-loading increased the aromatic yield. It was noticeable that if the Ni content increased further, the aromatic yield decreased.

Fig. 4c indicates the response surface of the aromatic yield is a function of the reaction time and temperature. A high level of reaction time and temperature increased the aromatic yield. These conditions caused the process to produce more aromatic compounds in the products. The optimum values of X_2 and X_3 were 120min for the

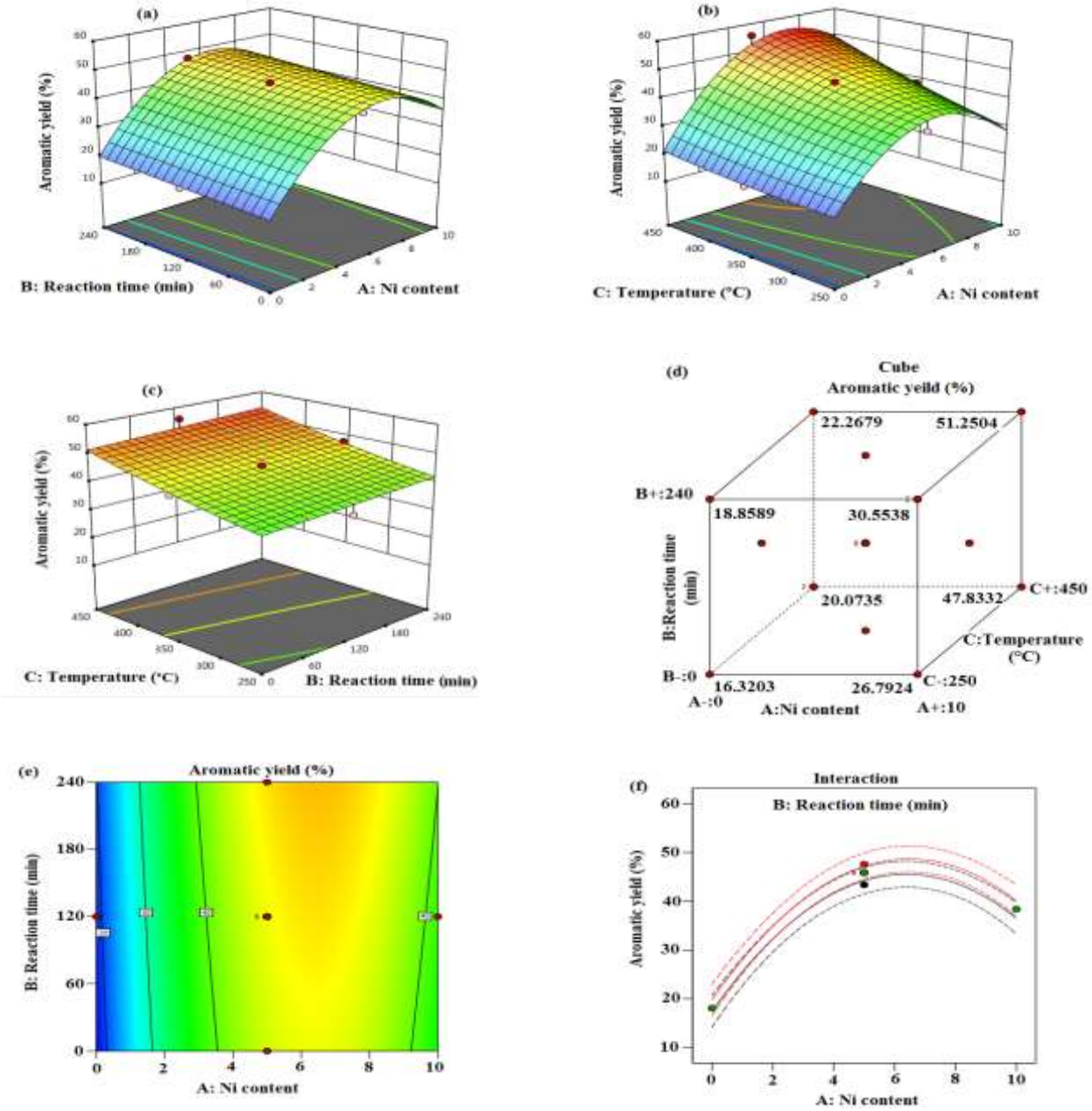

Fig. 4: Three-dimensional response surface plots for the effect of (a) reaction time and Ni content; (b) temperature and Ni content; (c) temperature and reaction time; (d) Ni content, reaction time, and temperature on the aromatic yield of the liquid products; (e) Contour graph as a function of Ni content and reaction time at constant temperature; (f) Interaction diagram of the model.

time reaction and 350ºC for temperature, respectively. The predicted value of aromatic yield was 52.62 in these conditions.

Fig. 4d indicates the distribution of aromatic yield on a cube model. The highest aromatic yield for the edge (51.25%) was achieved when the 10%Ni/HY was used at a temperature of 450ºC temperature and a reaction time of 240min.

However, as shown at the top center of the cubic model, the maximum aromatic yield (55.74%) was observed for conditions of a Ni content of 5%, a reaction time of 120min, and a temperature of 450ºC for the experiment.

Under these optimum conditions, the model predicted a maximum aromatic yield of around 52.62%. This value was due to a decrease in the stability of the Ni/HY catalyst when Ni content increased.

Fig. 4e shows the contour graph of the aromatic yield with Ni content and reaction time at a fixed temperature, and Fig. 4f indicates the interaction graph of parameters. These two figures represent the effect of the interactions between both factors of Ni content and reaction time on the aromatic yield.

The lowest content of aromatic obtained by the model (16.32%) occurred in homogeneous conditions. The aromatic content of none of the liquids produced over the Ni/HY catalysts was in the standard range of hydrocarbon fuels. This suggests that the development of an alternative method for the removal of aromatic compounds is necessary if the aim is the application of liquid products as a hydrocarbon fuel.

CONCLUSIONS

In this paper, nanostructured Ni/HY catalysts were first successfully synthesized through the deposition-precipitation method and then applied to the aromatization of kerosene in a fixed-bed reactor. A combination of the RSM (response surface method) and CCD (central composite design) was used to optimize the reaction parameters of the aromatic content of liquid products. According to the ANOVA analysis, the R_2 showed the highest confidence level (98.09%). The optimum conditions of aromatic yield occurred in the presence of 5% Ni content, a time reaction of 120min, and a temperature of 450ºC in which the maximum aromatic yield of kerosene obtained by the model was 52.62%. The metal content in the catalysts, which could change the route of the reforming process toward new reactions, was the most important independent variable. In this work, the aromatic yield increased as the Nickel content of the catalysts increased up to 5%; beyond that, a reduction in aromatic content was observed. Therefore, it is necessary to optimize the metal loading of the catalysts to achieve the desired value of components in hydrocarbon fuels. The results of RSM modeling are also useful to properly design the aromatization reaction to obtain the maximum aromatic content in products.

Abbreviations

ANOVA	Analysis of variance
ASTM	American society for testing and materials
CCD	Central composite design
FWHM	Full width at half maximum of the peak
GC-FID	Gas chromatography- flame ionization detector
ID	Internal diameter
JCPDS	Joint committee of powder diffraction standards
RSM	Response surface methodology
TORC	Tehran oil refinery company
XRD	X-ray diffraction

Received : Aug. 3, 2021 ; Accepted : Oct. 11, 2021

REFERENCES

[1] Ruan H., Qin Y., Heyne J., Gieleciak R., Fenga M., Yang B., Chemical Compositions and Properties of Lignin-Based Jet Fuel Range Hydrocarbons, *Fuel*, **256**: 115947 (2019).

[2] Osmont A., Gçkalp I., Evaluating Missile Fuels, *Prop. Explos. Pyrotech.*, **31**: 343–354 (2006).

[3] Liu G., Yan B., Chen G., Technical Review on Jet Fuel Production, *Renew. Sust. Energ. Rev.*, **25**: 59–70 (2013).

[4] Li J., Wang L., Zhang D., Qian J., Liu L., One‐Step Synthesis of Hierarchical ZSM‐5 Zeolites and Their Catalytic Performance on the Conversion of Methanol to Aromatics, *React. Kinet. Mech. Cat.*, **130**: 519–530 (2020).

[5] Escalona G., Rai A., Betancourt P., Sinha A.K. Selective Poly-Aromatics Saturation and Ring Opening During Hydroprocessing of Light Cycle Oil over Sulfided Ni-Mo/SiO_2-Al_2O_3 Catalyst, *Fuel*, **219**: 270-278 (2018).

[6] Sedighi M., Keyvanloo K., Towfighi J., Experimental Study and Optimization of Heavy Liquid Hydrocarbon Thermal Cracking to Light Olefins by Response Surface Methodology, *Korean J. Chem. Eng.*, **27(4)**: 1170-1176 (2010).

[7] Huang P., Zhang X.J., Mao X.F., Research on the Production of Aromatic Hydrocarbon *via* Hydroreforming a Light Fraction in Direct Coal Liquefaction Oil, *Energy Fuels*, **29**: 86–90 (2015).

[8] Khasanova E.I., Nazmieva I.F., Ziyatdinov A.S., Salakhov I.I., Kopylov A.Y. A Study of Propane Aromatization on a Zeolite-Containing Catalyst with Different Si/Al Ratios, *Petr. Chem.*, **52**: 79–85 (2012).

[9] Vosmerikov A.A., Vosmerikova L.N., Danilova I.G., Vosmerikov A.V., Production of Aromatic Hydrocarbons from C_3, C_4-Alkanes over Zeolite Catalysts, *J. Siber. Fed. Univer.*, **12**: 144–154 (2019).

[10] Popov A., Pavlov V., Ivanova I., Effect of Crystal Size on Butenes Oligomerization over MFI Catalysts, *Catal. J.*, **335**: 155-164 (2016).

[11] Qi S.C., Wei X.Y., Zong Z.M., Hayashi J., Yuan X.H., Sun L.B., A Highly Active Ni/ZSM-5 Catalyst for Complete Hydrogenation of Poly Methyl Benzenes, *Chem. Cat. Chem.*, **5**: 3543–3547 (2013).

[12] Kubička D., Černý R., Upgrading of Fischer-Tropsch Waxes by Fluid Catalytic Cracking, *Ind. Eng. Chem. Res.*, **51**: 8849–8857 (2012).

[13] Hassani M., Najafpour G. D., Mohammadi M., Rabiee M., Preparation, Characterization and Application of Zeolite-Based Catalyst for Production of Biodiesel from Waste Cooking Oil, *J. Sci. Ind. Res.*, **73**: 129–33 (2014).

[14] Thomas F., Degnan J., Applications of Zeolites in Petroleum Refining, *Top. Catal.*, **13**: 349–356 (2000).

[15] Li T., Cheng J., Huang R., Zhou J., Cen K., Conversion of Waste Cooking Oil to Jet Biofuel with Nickel-Based Mesoporous Zeolite Y Catalyst, *Bioresour. Technol*., **197**: 289–294 (2015).

[16] Lallemand M., Rusu O.A., Dumitriu E., Finiels A., Fajula F., Hulea V., NiMCM-36 and NiMCM-22 Catalysts for the Ethylene Oligomerization: Effect of Zeolite Texture and Nickel Cations/Acid Sites ratio, *Appl. Catal. A*, **338**: 37-43 (2008).

[17] Maia A.J., Louis B., Lam Y.L., Pereira M.M., Ni-ZSM-5 Catalysts: Detailed Characterization of Metal Sites for Proper Catalyst Design, *J. Catal*., **269**: 103–109 (2010).

[18] Goula M.A., Charisiou N.D., Papageridis K.N., Delimitis A., Pachatouridou E., Iliopoulou E.F., Nickel on Alumina Catalysts for the Production of Hydrogen Rich Mixtures via the Biogas Dry Reforming Reaction: Influence of the Synthesis Method, *Int. J. Hydrog. Energy*, **40**: 9183–9201 (2015).

[19] Daza C.E., Kiennemann A., Moreno S., Molina R., Dry Reforming of Methane using Ni–Ce Catalysts Supported on Modified Mineral Clay, *Appl. Catal. A*, **364**: 65–74 (2009).

[20] Coqueblina H., Richard A., Uzio D., Pinard L., Pouilloux Y., Epron F., Effect of the Metal Promoter on the Performances of H-ZSM5 in Ethylene Aromatization, *Catal. Today*, **289**: 62-69 (2017).

[21] Anunziata O.A., Cussa J., Beltramone A.R., Simultaneous Optimization of Methane Conversion and Aromatic Yields by Catalytic Activation with Ethane over Zn-ZSM-11 Zeolite: The Influence of the Zn-Loading Factor, *Catal. Today*, **171**: 36-42 (2011).

[22] Bezerra M.A., Santelli R.E., Oliveira E.P., Villar L.S., Escaleira L.A., Response Surface Methodology (RSM) as a Tool for Optimization in Analytical Chemistry, *Talanta*,**76**: 965–977 (2008).

[23] Nasouri K., Shoushtari A.M., Khamforoush M., Comparison between Artificial Neural Network and Response Surface Methodology in the Prediction of the Production Rate of Polyacrylonitrile Electrospun Nanofibers, *Fibers Polym.*, **14**: 1849–1856 (2013).

[24] Souza de Carvalho Filho J.F., Maciel Pereira M., Gomes Aranda D.A., Ribeiro de Almeida J.M.A., Sousa-Aguiar E.F. Nothaft Romano P., Application of Response Surface Methodology for Ethanol Conversion into Hydrocarbons using ZSM-5 Zeolites, *Catalysts*, **9**: 617–631 (2019).

[25] Box G., Wilson K., On the Experimental Attainment of Optimum Conditions, *J. R. Sta.t Soc. Series B Stat/ Methodol.*, **13**:1–45 (1951).

[26] Myers R.H., Montgomery D.C., Anderson-Cook C.M., "Response Surface Methodology. Process and Product Optimization using Designed Experiments", 4th ed. John Wiley & Sons, Inc. (2016).

[27] Mante O.D., Agblevor F.A., McClung., A Study on Catalytic Pyrolysis of Biomass with Y-Zeolite Based FCC Catalyst using Response Surface Methodology, *Fuel*, **108**:451–464 (2013).

[28] Sarve A., Sonawane S.S., Varma M.N., Ultrasound Assisted Biodiesel Production from Sesame (Sesamum Indicum L.) Oil using Barium Hydroxide as a Heterogeneous Catalyst: Comparative Assessment of Prediction Abilities between Response Surface Methodology (RSM) and Artificial Neural Network (ANN), *Ultrason. Sonochem*., **26**: 218–228 (2015).

[29] Srivatsa S.C., Li F., Bhattacharya S., Optimization of Reaction Parameters for Bio-Oil Production by Catalytic Pyrolysis of Microalga Tetraselmis Suecica: Influence of Ni-loading on the Bio-Oil Composition, *Renew. Energy*, **142**:426-436 (2019).

[30] Atashi H., Dinarvandi K., Zarintorang H., Mirzaei A.A., Modeling and Optimization of Fischer-Tropsch Petroleum Products on Silica-Cobalt Catalyst in Fix Bed Reactor, *Pet Sci Technol*, **38**:247-256 (2020).

[31] Chananipoor A., Azizi, Z., Raei B., Tahmasebi N., Synthesis and Optimization of GO/PMMA/n-Octadecane Phase Change Nanocapsules Using Response Surface Methodology, *Iran. J. Chem. Chem. Eng. (IJCCE)*, **40**(2**)**: 383-394 (2021).

[32] Li X., Chen Y, Hao Y., Zhang X., Du J., Zhang A., Optimization of Aviation Kerosene from One-Step Hydrotreatment of Catalytic Jatropha Oil over SDBS-Pt/SAPO-11 by Response Surface Methodology, *Renew. Energy*, **139**:551-559 (2019).

[33] Elfghi M.F., Amin N.A.S., Elgarni M. M., Optimization of Isomerization Activity and Aromatization Activity in Catalytic Naphtha Reforming over Tri-Metallic Modified Catalyst using Design of Experiment Based on Central Composite Design and Response Surface Methodology, *J. Adv. C, Sci. Technol. Catal.*, **2**: 1-17 (2015).

[34] Aghaziarati M., Soltanieh M., Kazemeini M., Khandan N., Synthesis of Tetrahydrofuran from Maleic Anhydride on Cu–ZnO–ZrO/H-Y Bifunctional Catalysts, *Catal. Commun.*, **9**: 2195-2200 (2008).

[35] Khandan N., Ziarati M., Karkeabadi R., Ghafouri Roozbahani M.A., Hydrogen Production via Steam Reforming of LPG on Ni/zeolite Catalysts, *Iran. J. Hydrog. Fuel Cell*, **4**:233-238 (2014).

[36] Takayasu T., Kondo T., Components of Gasoline and Kerosene, *Springer-Verlag Berlin Heidelberg*, 159-169 (2005).

[37] Fang W., Kittelson D.B., Northrop W.F., Optimization of Reactivity-Controlled Compression Ignition Combustion Fueled with Diesel and Hydrous Ethanol using Response Surface Methodology, *Fuel*, **160**: 446-457 (2015).

[38] Mante O.D., Agblevor F.A., McClung R., A Study on Catalytic Pyrolysis of Biomass with Y-Zeolite Based FCC Catalyst using Response Surface Methodology, *Fuel*, **108**:451-464 (2013).

[39] Alagar M., Theivasanthi T., Raja A.K., Chemical Synthesis of Nano-sized Particles of Lead Oxide and their Characterization Studies, *J. of App. Sci*., **12**: 398–401 (2012).

[40] Rifaya M.N., Theivasanthi T., Alagar M., Chemical Capping Synthesis of Nickel Oxide Nanoparticles and their Characterizations Studies, *Nanosci. Nanotechnol*, **2**:134–138 (2012).

[41] Theivasanthi T., Alagar M., An Insight Analysis of Nano Sized Powder of Jackfruit Seed, *Nano Biomed. Eng*., **3**:163–168 (2011).

[42] Gleiter H., Nanocrystalline Materials, *Prog. Mater. Sci.*, **33**: 223-315 (1989).

[43] Box G.E.P., Wilson K.B., "On the Experimental Attainment of Optimum Conditions", *In: Kotz S., Johnson N.L. (eds) Breakthroughs in Statistics. Springer Series in Statistics (Perspectives in Statistics). Springer, New York, NY.* (1992).